

Zeroing Control Barrier Functions for Safe Volitional Pedaling in a Motorized Cycle ^{*}

Axton Isaly^{*} Brendon C. Allen^{*}
Ricardo G. Sanfelice^{**} Warren E. Dixon^{*}

^{*} *Department of Mechanical and Aerospace Engineering, University of Florida, Gainesville FL 32611-6250, USA Email: {axtonisaly1013, brendoncallen, wdixon}@ufl.edu.*

^{**} *Department of Electrical and Computer Engineering, University of California, Santa Cruz. Email: ricardo@ucsc.edu.*

Abstract: A minimally restrictive robust controller is developed for a motorized rehabilitative cycling system. The controller yields a forced-use movement therapy that constrains the rider’s cadence to remain within a user-defined range. The controller is designed using a zeroing control barrier function (ZCBF), which facilitates the therapy by reducing control effort when the rider can sustain the desired cadence volitionally. Moreover, the ZCBF design approach certifies the rider’s safety by ensuring the desired cadence range is an asymptotically stable set. The effectiveness of the controller is demonstrated with a preliminary experimental result, which shows the cadence constrained within a range of 50 ± 8 RPM even when the rider stops pedaling volitionally mid-trial. Additionally, the rider was able to pedal with no intervention from the motor when volitional effort was present.

Keywords: Rehabilitative Cycling, Barrier Function, Safety-critical, Euler-Lagrange

1. INTRODUCTION

Motorized cycling is an effective tool for the rehabilitation of individuals with neuromuscular disorders Hooker et al. (1992); Rösche et al. (1997); Johnston et al. (2008). Automated cycling programs can assist physical therapists by using closed-loop control to yield safe, consistent, and accurate cycling repetitions despite uncertainty in the nonlinear human-machine dynamic system Kawai et al. (2019); Bellman et al. (2017). Results such as Duenas et al. (2018); Cousin et al. (2019) are robust to unknown, person-specific parameters such as muscle fatigue rate and power transfer ratio. Although successful forced-use therapy may require intermittent assistance from the motorized system, greater physiological benefits (e.g., increased heart rate and power output) are attained by allowing the rider to pedal using their volitional effort whenever a reasonable cadence can be sustained without assistance Harrington et al. (2012); Rouse et al. (2018); Combs et al. (2010). Thus, it is desirable to develop control strategies in which the motor is inactive within a range of prescribed therapeutic cadence values.

Rider safety is the most critical consideration when designing any automated therapy program. Potential dangers to the rider’s safety in forced-use therapy include uncontrolled or erratic cadences and control action from the motor that is excessive or abrupt. Barrier functions can be used to develop automatic controllers that ensure

a set of states (e.g., a safe range of cadence values) is forward invariant, meaning that trajectories starting in the set remain there for all of time Ames et al. (2019); Maghenem and Sanfelice (2018). However, some common barrier functions are undefined outside the set of interest, and therefore cannot certify safety for states outside the set Tee et al. (2009); Ames et al. (2016). In contrast, zeroing control barrier functions (ZCBFs) are defined on the entire state space and provide robust safety guarantees such as asymptotic stability Xu et al. (2015). Additionally, ZCBFs use minimal conditions for invariance to allow control effort to be relaxed for states within the set. Moreover, ZCBFs are applicable to dynamic systems with disturbances and unknown parameters Emam et al. (2019). The aforementioned results motivate investigating ZCBFs as a design method to facilitate the aims of safe, forced-use cycling within a desired cadence range with minimal control effort. Specifically, the objective of this paper is to develop an automated motor controller that ensures a user-defined range of cadence values is uniformly globally asymptotically stable (UGAS).

In our related work in Rouse et al. (2020), we developed a hybrid controller that switched between the cycle motor and functional electrical stimulation (FES) of the rider’s lower-limb muscle groups to establish controlled regions outside of the desired cadence range, while no controller was applied when the rider pedaled within the desired cadence region. In contrast, the ZCBF control method in this paper is applied with minimal interaction near the midpoint of the cadence range, with increasing control effort near the boundary. This approach guarantees forward invariance of the specified range, and encourages

^{*} This research is supported in part by AFOSR award number FA9550-19-1-0169 and NSF Award number 1762829. Any opinions, findings and conclusions or recommendations expressed in this material are those of the author(s) and do not necessarily reflect the views of the sponsoring agency.

rider effort because the cadence cannot be sustained at the midpoint without volitional input. While this paper only considers control efforts by the cycle motor, future extensions can incorporate additional FES inputs following the work in results such as Rouse et al. (2020, 2019). To account for the unknown dynamics and time-varying disturbances in rehabilitative cycling, we show how traditional ZCBF methods can be generalized to incorporate Lyapunov-based robust control tools. Moreover, we construct an explicit control law that ensures the existence of a ZCBF while solving a min-norm quadratic program (QP). The controller was developed in Xu et al. (2015) under a stronger regularity condition than the one used here. The controller is locally Lipschitz continuous on the entire state space. A preliminary experimental trial shows that, despite intentional disruptions in the volitional effort, the cadence is constrained within a desired range of 42 to 58 RPM. When volitional effort is present, there is no input from the motor during a 30-second segment of cycling. Additional experiments are in progress.

2. MODEL

The dynamics of the motorized cycle-rider system are Bellman et al. (2017)

$$\begin{aligned} M(q)\ddot{q} + \tau_b(\dot{q}) + V_p(q, \dot{q})\dot{q} + G(q) + P(q, \dot{q}) + \tau_d(t) \\ = \tau_e(t) + \tau_{vol}(t) \end{aligned} \quad (1)$$

where ¹ $q : \mathbb{R}_{>0} \rightarrow \mathbb{R}$ denotes the cycle's measurable crank angle, $\dot{q} : \mathbb{R}_{>0} \rightarrow \mathbb{R}$ is the measurable angular velocity, and $\ddot{q} : \mathbb{R}_{>0} \rightarrow \mathbb{R}$ is the angular acceleration. The effects of inertial, centripetal-Coriolis, gravitational, and passive viscoelastic tissue forces in both the cycle and the rider's limbs are denoted by $M : \mathbb{R} \rightarrow \mathbb{R}_{>0}$, $V_p : \mathbb{R}^2 \rightarrow \mathbb{R}$, $G : \mathbb{R} \rightarrow \mathbb{R}$, and $P : \mathbb{R}^2 \rightarrow \mathbb{R}$, respectively. The unknown torque due to viscous damping is denoted by $\tau_b : \mathbb{R} \rightarrow \mathbb{R}$, and $\tau_d : \mathbb{R}_{>0} \rightarrow \mathbb{R}$ denotes disturbances from effects such as spasticity or changes in load. The rider's volitional torque is denoted by $\tau_{vol} : \mathbb{R}_{>0} \rightarrow \mathbb{R}$, and the torque produced by the electric motor is $\tau_e : \mathbb{R}_{>0} \rightarrow \mathbb{R}$. The control input is designed in terms of the motor torque, which can be related to the current input to the motor, $u_e : \mathbb{R}_{>0} \rightarrow \mathbb{R}$, with $\tau_e(t) = B_e u_e(t)$, where $B_e \in \mathbb{R}_{>0}$. The following properties of the cycle-rider system in (1) are derived from a detailed dynamic model, as discussed previously in Bellman et al. (2017).

Property 1. The inertial term is smooth (i.e. infinitely differentiable), and can be lower- and upper-bounded as $c_m \leq M(q) \leq c_M$, where $c_m, c_M \in \mathbb{R}_{>0}$ are known constants. *Property 2.* $|V_p(q, \dot{q})| \leq c_V |\dot{q}|$, where $c_V \in \mathbb{R}_{>0}$ is a known constant. *Property 3.* $|G(q)| \leq c_G$, where $c_G \in \mathbb{R}_{>0}$ is a known constant. *Property 4.* $|P(q, \dot{q})| \leq c_{P1} + c_{P2} |\dot{q}|$, where $c_{P1}, c_{P2} \in \mathbb{R}_{>0}$ are known constants. *Property 5.* $|\tau_b(\dot{q})| \leq c_b |\dot{q}|$, where $c_b \in \mathbb{R}_{>0}$ is a known constant. *Property 6.* $|\tau_d(t)| \leq c_d$, where $c_d \in \mathbb{R}_{>0}$ is a known constant. *Property 7.* $|\tau_{vol}(t)| \leq c_{vol}$, where $c_{vol} \in \mathbb{R}_{>0}$ is a known constant. *Property 8.* $\frac{1}{2}\dot{M}(q) = V_p(q, \dot{q})$.

¹ $\mathbb{R}_{>0}$ indicates strictly positive real numbers while $\mathbb{R}_{\geq 0}$ indicates non-negative reals.

To facilitate the subsequent development, we define $z \triangleq [q, \dot{q}]^T$ and use Property 1 to rewrite the dynamic model in (1) as

$$\begin{bmatrix} \dot{z}_1 \\ \dot{z}_2 \end{bmatrix} = \underbrace{\begin{bmatrix} z_2 \\ M^{-1}(z_1)\tau_f(z, d(t)) \end{bmatrix}}_{f(z, d(t))} + \underbrace{\begin{bmatrix} 0 \\ M^{-1}(z_1) \end{bmatrix}}_{g(z)} \tau_e, \quad (2)$$

where $\tau_f : \mathbb{R}^2 \times \Omega \rightarrow \mathbb{R}$ is an auxiliary term defined as

$$\begin{aligned} \tau_f(z, d(t)) \triangleq d(t) - [\tau_b(z_2) + V_p(z)z_2 \\ + G(z_1) + P(z)], \end{aligned} \quad (3)$$

and the volitional effort and system disturbances are modeled by a continuous, unknown, time-dependent disturbance $d : \mathbb{R}_{\geq 0} \rightarrow \Omega$ as

$$d(t) \triangleq \tau_{vol}(t) - \tau_d(t). \quad (4)$$

Properties 6 and 7 imply that the range of the disturbance term, $\Omega \subset \mathbb{R}$, is compact.

Property 9. In (2), the function $g(z)$ is globally Lipschitz in z . The function $f(z, d(t))$ is locally Lipschitz in z and, on any convex subset of \mathbb{R}^2 for which z_2 is bounded, is Lipschitz in z for all $t \geq 0$. These properties are developed using the fact that all dependencies on the state z_1 are embedded in trigonometric functions Bellman et al. (2017).

3. CONTROL DEVELOPMENT

3.1 Control Objective and Barrier Function Selection

The control objective is to constrain the rider's cadence within a user-defined range about a constant setpoint. This objective is quantified by defining the tracking error as

$$e \triangleq z_{2d} - z_2, \quad (5)$$

where $z_{2d} \in \mathbb{R}_{>0}$ is a user-defined desired cadence. The goal is to constrain the tracking error so that $e \in [-\Delta_d, \Delta_d]$, where $\Delta_d \in \mathbb{R}_{>0}$ defines the desired cadence range. As a secondary objective, the motor control effort should be small for small tracking errors so that the rider is forced to pedal volitionally to maintain the target cadence of z_{2d} . ZCBFs are well suited for accomplishing the aforementioned control objectives. In addition, ZCBFs will guarantee the safety of the rider by ensuring asymptotic stability of the desired cadence range, which results in robustness properties as detailed in Xu et al. (2015). To motivate the subsequent ZCBF-based analysis, consider the following definition.²

Definition 1. Consider a smooth function $h : \mathbb{R}^2 \rightarrow \mathbb{R}$ and the safe set \mathcal{S} defined as $\mathcal{S} \triangleq \{z \in \mathbb{R}^2 : h(z) \leq 0\}$. The function h is a ZCBF for the dynamic system in (2) if there exist a set \mathcal{D} with $\mathcal{S} \subseteq \mathcal{D} \subseteq \mathbb{R}^2$ and an extended class \mathcal{K} function³ α such that

$$\inf_{\tau_e \in \mathbb{R}} \left[\frac{\partial h}{\partial z} f(z, d(t)) + \frac{\partial h}{\partial z} g(z) \tau_e \right] \leq -\alpha(h(z)), \quad (6)$$

for all $z \in \mathcal{D}$ and $t \geq 0$.

² The definition of a ZCBF for the disturbed system in (2) is based on Xu et al. (2015). Inspired by conventions associated with Lyapunov-based analysis methods, we define the safe set by the negative values of the ZCBF candidate.

³ An *extended class \mathcal{K} function* is defined as a continuous function $\beta : (-b, a) \rightarrow (-\infty, \infty)$ for some $a, b > 0$ that is strictly increasing and $\beta(0) = 0$ Xu et al. (2015).

Given additional assumptions, the existence of a ZCBF implies there exists a control input that renders the set \mathcal{S} either forward invariant or asymptotically stable. Following from Maghenem and Sanfelice (2018) and Lin et al. (1996), we provide conditions in Corollary 1 of the Appendix for the set \mathcal{S} to have these properties for a closed-loop system. Notice that (6) implies that the ZCBF may increase for states inside the safe set, which permits control effort relaxation.

Motivated by the subsequent analysis, we encode the cycling control objective by defining the ZCBF candidate

$$h(z) \triangleq \frac{1}{2}M(z_1)(e^2 - \Delta_d^2), \quad (7)$$

where the safe set is

$$\begin{aligned} \mathcal{S} &= \{z \in \mathbb{R}^2 : |e| \leq \Delta_d\} \\ &= \mathbb{R} \times [z_{2d} - \Delta_d, z_{2d} + \Delta_d]. \end{aligned} \quad (8)$$

The term $M(z_1)$ is included in (7) to compensate for the unknown term in the control effectiveness matrix $g(z)$ in (2). Using Property 1, it can be shown that $h(z)$ is smooth.

3.2 Safety Constraint Development

ZCBFs induce a constraint on the control input of the system. Using this constraint, we can construct a continuous controller that ensures safety while minimizing the magnitude of the motor control input. Our goal is to apply Corollary 1 in the Appendix, which requires finding any control input with which we can show that (6) holds.

To compensate for the unknown dynamics and time-varying disturbances present in the model in (2), Lyapunov-based robust control methods typically use a worst-case bound of the unknown terms. We will show that a similar procedure can be conducted in a ZCBF-based design to arrive at a conservative constraint that is sufficient for satisfaction of (6). Considering the system in (2) and the ZCBF candidate in (7), we compute:

$$\frac{\partial h}{\partial z} f(z, d(t)) = \frac{1}{2} \dot{M}(z_1)(e^2 - \Delta_d^2) - e\tau_f(z, d(t)), \quad (9)$$

$$\frac{\partial h}{\partial z} g(z) = -e. \quad (10)$$

Using Property 8 and making cancellations, the dynamics in (9) are written as

$$\begin{aligned} \frac{\partial h}{\partial z} f(z, d(t)) &= -V_p(z)\Delta_d^2 - e[d(t) - \tau_b(z_2) \\ &\quad - V_p(z)z_{2d} - G(z_1) - P(z)]. \end{aligned} \quad (11)$$

Using Properties 2-7, the dynamics can be upper bounded as

$$\frac{\partial h}{\partial z} f(z, d(t)) \leq \bar{h}_C(e) \quad \forall z \in \mathbb{R}^2, t \geq 0, \quad (12)$$

where

$$\bar{h}_C(e) \triangleq C_1 + C_2|e| + C_3e^2,$$

and $C_1, C_2, C_3 \in \mathbb{R}_{>0}$ are known positive constants. To facilitate the subsequent control design, we also define

$$\bar{h}_K(e) \triangleq K_1 + K_2|e| + K_3e^2,$$

where $K_1, K_2, K_3 \in \mathbb{R}_{>0}$ are user-defined control gains selected so that

$$\bar{h}_C(e) \leq \bar{h}_K(e) \quad \forall e \in \mathbb{R}. \quad (13)$$

From (10), (12), and (13) it follows that

$$\frac{\partial h}{\partial z} f(z, d(t)) + \frac{\partial h}{\partial z} g(z)\tau_e \leq \bar{h}_K(e) - e\tau_e, \quad (14)$$

for all $z \in \mathbb{R}^2$ and $t \geq 0$.

Controllers based on Definition 1 frequently use the value of the ZCBF explicitly in the control law; however, $M(z_1)$ in (7) is unknown. We will consequently use a substitute function in the developed control law as an indicator of the distance to the boundary of the safe set. This substitute function is defined as

$$h_s(e) \triangleq K_b(e^2 - \Delta_d^2), \quad (15)$$

where $K_b \in \mathbb{R}_{>0}$ is an additional control gain. In the subsequent stability analysis, we will find an extended class \mathcal{K} function α so that $\alpha(h(z))$ lower bounds $h_s(e)$. Considering Definition 1 with $\mathcal{D} = \mathbb{R}^2$, and using the bound developed in (14), satisfaction of the following inequality for all $e \in \mathbb{R}$ implies that h in (7) is a ZCBF:

$$\bar{h}_K(e) - e\tau_e \leq -h_s(e). \quad (16)$$

Specifically, given (13), condition (6) will hold at any point for which (16) holds. When $e = 0$, the constraint in (16) cannot be influenced by the control input. The following result, which follows immediately from (16), will allow selection of a minimal control at and around the point $e = 0$.

Lemma 1. For all $e \in \mathbb{R}$ such that $h_s(e) + \bar{h}_K(e) \leq 0$, the inequality in (16) is satisfied with $\tau_e = 0$.

Using the fact that h_s and \bar{h}_K are continuous, we can ensure that $h_s(e) + \bar{h}_K(e) \leq 0$ in a neighborhood about the point $e = 0$ by requiring the following strict inequality to hold:

$$h_s(0) + \bar{h}_K(0) = K_1 - K_b\Delta_d^2 < 0. \quad (17)$$

Because the terms in (17) are user-selected, they can be designed so the inequality holds.

3.3 Control Design

In this application, we wish to turn the motor off whenever possible while still ensuring safety. Following Lemma 1, we design a control law that sets $\tau_e = 0$ whenever this input satisfies the inequality in (16). The following controller will be shown to satisfy (16) with minimal control effort:

$$\tau_e^*(e) = \begin{cases} \tau_{con}(e) & h_s(e) + \bar{h}_K(e) > 0 \\ 0 & \text{otherwise,} \end{cases} \quad (18)$$

where

$$\tau_{con}(e) \triangleq \frac{h_s(e) + \bar{h}_K(e)}{e} \quad \forall e \neq 0. \quad (19)$$

We emphasize that because the parameters in (17) are user-selected, there is a tuneable neighborhood about the point $e = 0$ where $\tau_e^*(e) = 0$. The controller in (18) for various gain selections satisfying (17) is shown in Figure 1.

The following lemma and the stability result in Section 4 show that the controller in (18) meets all of the control objectives for the system. Namely, it constrains the cadence to the desired range using minimal control effort, thereby ensuring the rider's safety while encouraging volitional pedaling. A closed-form solution to a comparable min-norm QP based on ZCBFs was developed in Theorem 8 of Xu et al. (2015) under an assumption which, in this work, corresponds to $\frac{\partial h}{\partial z} g(z) \neq 0$ for all $z \in \mathbb{R}^2$. The alternate construction presented here highlights the challenge of relaxing this assumption.

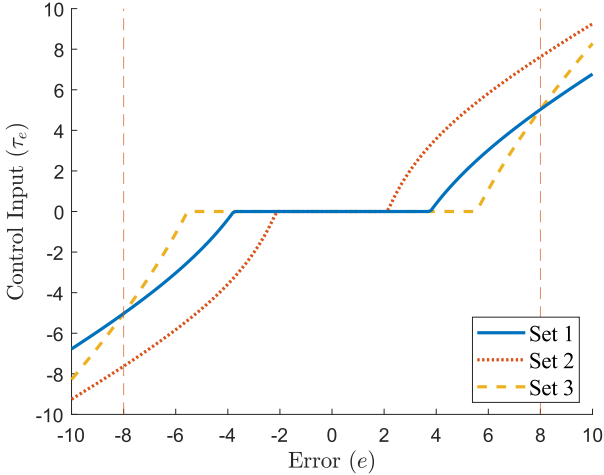


Fig. 1. Control input from the controller in (18) as a function of e for various sets of control gains that satisfy (17). Compared to Set 1, Set 2 had larger values for K_1 and K_2 . In Set 3, K_b was larger than in Set 1 while the other terms were the same. The dashed vertical lines represent the boundary of the safe range, where $\Delta_d = 8$.

Lemma 2. Assume that the gain condition in (17) holds. Then the controller τ_e^* in (18) solves the following QP:

$$\tau_e^*(e) = \arg \min_{\tau_e \in \mathbb{R}} \tau_e^2 \quad (20)$$

$$\text{s.t. } \bar{h}_K(e) - e\tau_e \leq -h_s(e).$$

Furthermore, the controller τ_e^* is locally Lipschitz on \mathbb{R} , and there exists a neighborhood $U(0)$ about the point $e = 0$ such that $\tau_e^*(e) = 0$ for all $e \in U(0)$.

Proof. We will show that the controller τ_e^* satisfies the constraint in (20) while minimizing the objective function. Choose $e \in \mathbb{R}$ such that $h_s(e) + \bar{h}_K(e) \leq 0$. From (18), $\tau_e^*(e) = 0$, which clearly minimizes the objective function. Moreover, Lemma 1 shows that the constraint is satisfied. Now choose $e \in \mathbb{R}$ such that $h_s(e) + \bar{h}_K(e) > 0$. Note that (17) ensures that $e \neq 0$ in this case. From (18) and (19), the constraint in (20) is satisfied since $\tau_e^*(e) = \tau_{con}(e)$ and

$$\bar{h}_K(e) - e\tau_{con}(e) = -h_s(e).$$

Furthermore, there is no $\tau_{e,2} \in \mathbb{R}$ with $\tau_{e,2}^2 < \tau_{con}^2(e)$ that satisfies the constraint. Indeed, because $e\tau_{con}(e)$ is positive when $h_s(e) + \bar{h}_K(e) > 0$, one can find that $-e\tau_{e,2} > -e\tau_{con}(e)$ for any such $\tau_{e,2}$. Then,

$$\bar{h}_K(e) - e\tau_{e,2} > \bar{h}_K(e) - e\tau_{con}(e) = -h_s(e),$$

which shows that $\tau_{e,2}$ does not satisfy the constraint. It follows that $\tau_e^*(e)$ solves the QP in (20) for every $e \in \mathbb{R}$.

To prove the final claims of the lemma, first notice that because the functions h_s and \bar{h}_K are continuous and $h_s(0) + \bar{h}_K(0) < 0$, there exists a neighborhood $U(0)$ about the point $e = 0$ for which $h_s(e) + \bar{h}_K(e) < 0$ for all $e \in U(0)$. From (18), $\tau_e^*(e) = 0$ for all $e \in U(0)$. It then follows from the definition of a locally Lipschitz function and the fact that $e \mapsto 0$ is locally Lipschitz that $\tau_e^*(e)$ is locally Lipschitz at $e = 0$. The argument that $\tau_e^*(e)$ is locally Lipschitz for all $e \in \mathbb{R}$ now follows from arguments made in the proof of Theorem 8 in Xu et al. (2015). \square

Remark 1. The controller in (18) can be rewritten as

$$\tau_e^*(e) = \begin{cases} \tau_{con}(e) & |e| > \beta \\ 0 & \text{otherwise,} \end{cases}$$

where $\beta > 0$ is guaranteed to exist when (17) is satisfied. In fact, β can be determined by finding the roots of the expression

$$h_s(e) + \bar{h}_K(e) = (K_3 + K_b)e^2 + K_2|e| + (K_1 - K_b\Delta_d^2).$$

4. STABILITY ANALYSIS

The Appendix contains a definition of UGAS and Corollary 1, which will be used in the following theorem to show that the set \mathcal{S} in (8) is UGAS.

Theorem 1. Consider the the cycle-rider system in (2) subjected to the control input in (18). The safe set \mathcal{S} given in (8) is UGAS for the closed-loop system provided that the control gains satisfy (13) and (17).

Proof. Consider the ZCBF candidate h , as defined in (7). Using Lemma 2, the bound in (14), and the gain conditions in (13) and (17), it follows that the control law in (18) ensures that

$$\frac{\partial h}{\partial z} f(z, d(t)) + \frac{\partial h}{\partial z} g(z) \tau_e^*(e) \leq -h_s(e), \quad (21)$$

for all $z \in \mathbb{R}^2$ and $t \geq 0$. Let the extended class \mathcal{K} function α be defined as

$$\alpha(s) \triangleq \begin{cases} \frac{K_b}{c_M} s & s \geq 0 \\ \frac{2K_b}{c_m} s & s < 0. \end{cases}$$

Using Property 1, it can be shown that $\alpha(h(z)) \leq h_s(e)$ for all $z \in \mathbb{R}^2$. Combining the preceding inequality with (21) leads to (22) in Corollary 1. We therefore conclude that h in (7) is a ZCBF for the dynamic model in (2) on \mathbb{R}^2 . Note also that h is radially unbounded with respect to \mathcal{S} . To apply Corollary 1, it remains to show that each maximal solution to the closed-loop system is complete, which is non-trivial since \mathcal{S} is not compact.

Before proving completeness of solutions, we will first show some boundedness properties of trajectories. Using (21), we find that for any trajectory, the distance of the state $z_2(t)$ from \mathcal{S} is bounded. Since z_2 takes bounded values in \mathcal{S} , we conclude that $z_2(t)$ is bounded, i.e. $z_2(t) \in \mathcal{L}_\infty$, which implies that $e(t), h(e(t)), h_s(e(t)) \in \mathcal{L}_\infty$. From boundedness of $e(t)$ and continuity of the controller τ_e^* it follows that $\tau_e^*(e(t)) \in \mathcal{L}_\infty$. Let $z : \text{dom } z \rightarrow \mathbb{R}^2$ be a solution to the closed-loop system with domain of definition $\text{dom } z \subseteq [0, \infty)$. Property 9, local Lipschitz continuity of the controller, and boundedness of $z_2(t)$ imply that there exists an open, convex set $W \subset \mathbb{R}^2$ on which the closed-loop dynamics are Lipschitz in z , uniformly in time, and $z(t) \in W$ for all $t \in \text{dom } z$. Therefore, for any time $t_0 \in \text{dom } z$, Theorem 3.1 in Khalil (2002) can be applied to find that the solution is defined on the interval $[t_0, t_0 + \delta]$ for some $\delta > 0$. Since $z(t_0 + \delta) \in W$, the procedure can be repeated indefinitely to find that $\text{dom } z$ is unbounded. It follows that every maximal solution is complete. Corollary 1 can now be used

to conclude that the set \mathcal{S} is UGAS. From the definition of UGAS, we have that $\|e(t)\|_{\mathcal{S}} \rightarrow 0$ as $t \rightarrow \infty$ and, again by definition, if $e(0) \in \mathcal{S}$ then $e(t) \in \mathcal{S}$ for all $t \geq 0$ (i.e. \mathcal{S} is forward invariant). \square

5. EXPERIMENTS

Experiments were conducted to evaluate the controller in (18) in terms of its effectiveness both at maintaining the desired cadence range and relaxing the control input when volitional effort is sufficient. Experiments were performed on an able-bodied person who gave written informed consent approved by the University of Florida Institutional Review Board.

5.1 Motorized Cycling Testbed

The experimental testbed consisted of a modified recumbent tricycle (TerraTrike Rover) with a 250 W, 24 V motor (Unite Motor Co.) coupled to the drive chain. To measure position and cadence, an optical encoder with an angular resolution of 20,000 pulses per revolution (US Digital H1) was mounted to the crank using spur gears. A desktop computer running real-time control software (QUARC integrated with Simulink) was used to interface the encoder and motor through a data acquisition board (Quanser Q-PIDe) at a sampling rate of 500 Hz. For additional safety, an emergency stop switch was mounted on the cycle to allow the participant to end the experiment if required. Further details are available in Rouse et al. (2020).

5.2 Experimental Procedure

The participant was asked to pedal according to a predetermined pattern. During an initial ramp-up, the motor was used to bring the rider's cadence to the setpoint, $z_{2d} = 50$ RPM, through a smooth trajectory, during which the rider could sit passively. The participant was then asked to provide volitional inputs to the best of their ability for approximately 30 seconds. The participant was then asked to stop all volitional effort for 20 seconds. Finally, the participant was asked to attempt to pedal faster than the upper cadence limit for 20 seconds. Throughout the experiment, the participant could view their cadence and the boundaries of the cadence range on a screen. The desired range Δ_d was set to 8 RPM so that the ZCBF encodes a range of cadence values given by $z_2 \in [42, 58]$ RPM. The control gains for the experiment were $K_b = 3.0$, $K_1 = 0.5$, $K_2 = 1.5$, and $K_3 = 3.5$. The tracking error e was converted from units of RPM to rad/s before computing the control input using (18).

5.3 Results

The cadence and motor current from all three segments (not including the ramp-up) of the experimental trial are displayed in Figure 2. Note that the amperage offset during the first segment of testing, when the rider was pedaling volitionally, is due to EMF induced current in the motor and not due to any motor control command. The control input was zero for effectively the entire first segment of testing. The cadence did not exit the user-defined range for the duration of the experiment. The minimum cadence

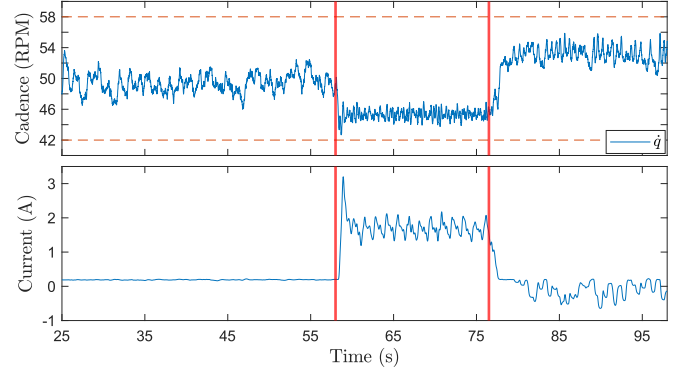


Fig. 2. Cadence of an able-bodied rider (top) and delivered motor current (bottom). The dashed horizontal lines represent the upper and lower limits of the user-defined cadence range. The vertical red lines indicate times at which the rider was asked to change their objective. The motor current has been filtered with a 0.5 s moving average for clarity. The initial 25 s ramp up phase has been excluded.

during the trial was 42.7 RPM, and the maximum was 55.9 RPM. The minimum cadence occurred after the rider abruptly stopped pedaling at the beginning of the second segment of the trial.

5.4 Discussion

The performance of the controller in (18) can be significantly altered by adjusting the tunable parameters. The size of the motor inactive region can be made smaller by increasing the terms K_1 and K_2 , as in the second gain set in Figure 1, so that control action is initiated at smaller error values. Alternately, the controller can be made stiffer by increasing the gains K_b and K_3 . In the third gain set in Figure 1, the barrier function gain K_b is increased, which has the effect of reducing control effort within the safe set and increasing it outside the boundary. However, the slope of the control signal is greater.

6. CONCLUSION

This paper used a ZCBF to design a nonrestrictive controller for a motorized cycle-rider system that ensures the rider's cadence remains within a user-defined set despite uncertain dynamics and disturbances. It was shown that a ZCBF induces a constraint on the control input of the system and an explicit control law was developed to ensure constraint satisfaction. Sufficient gain conditions were given that ensure the safe set is UGAS and the controller is locally Lipschitz continuous. Experimental results show that the safe set is forward invariant with a minimum distance of 0.7 RPM to the boundary of the set.

Future work will conduct a comprehensive experimental evaluation of the controller as a tool for rehabilitation. We also intend to integrate functional electrical stimulation (FES) into the cycling controller to increase its rehabilitative potential. Incorporating FES will require considering hybrid dynamics due to the switched nature of a combined motor and FES control system.

APPENDIX

In the following, a controller $\tau_e : \mathbb{R}^2 \rightarrow \mathbb{R}$ applied to the dynamic system in (2) defines a closed-loop system. A maximal solution $z : \text{dom } z \rightarrow \mathbb{R}^2$ to the closed-loop system is complete if its domain of definition $\text{dom } z \subseteq [0, \infty)$ is unbounded. A function $h : \mathbb{R}^2 \rightarrow \mathbb{R}$ is radially unbounded with respect to a set \mathcal{A} if $h(z) \rightarrow \infty$ as $\|z\|_{\mathcal{A}} \rightarrow \infty^4$.

Definition 2. A set $\mathcal{A} \subset \mathbb{R}^2$ is forward invariant for a closed-loop system if, for each maximal solution with initial state $z(0) \in \mathcal{A}$, $z(t) \in \mathcal{A}$ for all $t \geq 0$; see Maghenem and Sanfelice (2018).

Definition 3. A closed and forward invariant set $\mathcal{A} \subset \mathbb{R}^2$ is uniformly globally asymptotically stable (UGAS) for a closed-loop system if there exists a class \mathcal{KL} function β such that for each maximal solution with initial state $z(0) \in \mathbb{R}^2$, $\|z(t)\|_{\mathcal{A}} \leq \beta(\|z(0)\|_{\mathcal{A}}, t)$ for all $t \geq 0$; see Lin et al. (1996).

In the subsequent corollary, the conditions for forward invariance are developed using Theorem 1 in Maghenem and Sanfelice (2018). The conditions for UGAS are developed using Proposition 4.2 and then Theorem 2.8 in Lin et al. (1996).

Corollary 1. Consider the closed-loop system defined by a locally Lipschitz controller $\tau_e : \mathbb{R}^2 \rightarrow \mathbb{R}$ applied to the dynamic system in (2). Consider a smooth function $h : \mathbb{R}^2 \rightarrow \mathbb{R}$ and the safe set \mathcal{S} defined as $\mathcal{S} \triangleq \{z \in \mathbb{R}^2 : h(z) \leq 0\}$. If there exists an extended class \mathcal{K} function α and a set \mathcal{D} such that

$$\frac{\partial h}{\partial z} f(z, d(t)) + \frac{\partial h}{\partial z} g(z) \tau_e(z) \leq -\alpha(h(z)) \quad (22)$$

for all $z \in \mathcal{D}$ and $t \geq 0$, then h is a ZCBF for (2) on \mathcal{D} . Assume additionally that each maximal solution to the closed-loop system is complete. If \mathcal{D} is open, then the set \mathcal{S} is forward invariant for the closed-loop system. If $\mathcal{D} = \mathbb{R}^2$ and h is radially unbounded with respect to \mathcal{S} , then the set \mathcal{S} is UGAS for the closed-loop system.

REFERENCES

- Ames, A.D., Coogan, S., Egerstedt, M., Notomista, G., Sreenath, K., and Tabuada, P. (2019). Control barrier functions: Theory and applications. In *Proc. Eur. Control Conf.*, 3420–3431. IEEE.
- Ames, A.D., Xu, X., Grizzle, J.W., and Tabuada, P. (2016). Control barrier function based quadratic programs for safety critical systems. *IEEE Trans Autom Control*, 62(8), 3861–3876.
- Bellman, M.J., Downey, R.J., Parikh, A., and Dixon, W.E. (2017). Automatic control of cycling induced by functional electrical stimulation with electric motor assistance. *IEEE Trans. Autom. Science Eng.*, 14(2), 1225–1234. doi:10.1109/TASE.2016.2527716.
- Combs, S., Kelly, S., Barton, R., Ivaska, M., and Nowak, K. (2010). Effects of an intensive, task-specific rehabilitation program for individuals with chronic stroke: a case series. *Disabil. Rehabil.*, 32(8), 669–78.
- Cousin, C.A., Rouse, C.A., Duenas, V.H., and Dixon, W.E. (2019). Controlling the cadence and admittance of a functional electrical stimulation cycle. *IEEE Trans. Neural Syst. Rehabil. Eng.*, 27(6), 1181–1192.
- Duenas, V.H., Cousin, C., Ghanbari, V., and Dixon, W.E. (2018). Passivity-based learning control for torque and cadence tracking in functional electrical stimulation FES induced cycling. In *Proc. Am. Control Conf.*, 3726–3731.
- Emam, Y., Glotfelter, P., and Egerstedt, M. (2019). Robust barrier functions for a fully autonomous, remotely accessible swarm-robotics testbed. In *Proc. IEEE Conf. Decis. Control*, 3984–3990. IEEE.
- Harrington, A.T., McRae, C.G.A., and Lee, S.C.K. (2012). Evaluation of functional electrical stimulation to assist cycling in four adolescents with spastic cerebral palsy. *J. Pediatr.*, 2012, 1–11. doi:10.1155/2012/504387.
- Hooker, S.P., Figoni, S.F., Rodgers, M.M., Glaser, R.M., Mathews, T., Suryaprasad, A.G., and Gupta, S.C. (1992). Physiologic effects of electrical stimulation leg cycle exercise training in spinal cord injured persons. *Arch. Phys. Med. Rehabil.*, 73(5), 470–476.
- Johnston, T., Smith, B., Oladeji, O., Betz, R., and Lauer, R. (2008). Outcomes of a home cycling program using functional electrical stimulation or passive motion for children with spinal cord injury: a case series. *J. Spinal Cord Med.*, 31(2), 215–21.
- Kawai, H., Bellman, M., Downey, R., and Dixon, W.E. (2019). Closed-loop position and cadence tracking control for FES-cycling exploiting pedal force direction with antagonistic bi-articular muscles. *IEEE Trans. Control Syst. Tech.*, 27(2), 730–742.
- Khalil, H.K. (2002). *Nonlinear Systems*. Prentice Hall, Upper Saddle River, NJ, 3 edition.
- Lin, Y., Sontag, E.D., and Wang, Y. (1996). A smooth converse lyapunov theorem for robust stability. *SIAM J. Control Optim.*, 34(1), 124–160.
- Maghenem, M. and Sanfelice, R.G. (2018). Barrier function certificates for forward invariance in hybrid inclusions. In *Proc. IEEE Conf. Decis. Control*, 759–764.
- Rösche, J., Paulus, C., Maisch, U., Kaspar, A., Mauch, E., and Kornhuber, H. (1997). The effects of therapy on spasticity utilizing a motorized exercise-cycle. *Spinal cord*, 35(3), 176–178.
- Rouse, C., Cousin, C., Allen, B.C., and Dixon, W.E. (2019). Split-crank cadence tracking for switched motorized FES-cycling with volitional pedaling. In *Proc. Am. Control Conf.*, 4393–4398.
- Rouse, C., Cousin, C.A., Duenas, V., and Dixon, W.E. (2018). FES and motor assisted cycling to track power and cadence to desired voluntary bounds. In *Proc. IFAC Conf. Cyber. Phys. Hum. Syst.*, 34–39.
- Rouse, C., Downey, R., Gregory, C., Cousin, C., Duenas, V., and Dixon, W.E. (2020). FES cycling in stroke: Novel closed-loop algorithm accommodates differences in functional impairments. *IEEE Trans. Biomed. Eng.*, 67(3), 738–749.
- Tee, K.P., Ge, S.S., and Tay, E.H. (2009). Barrier lyapunov functions for the control of output-constrained nonlinear systems. *Automatica*, 45(4), 918–927.
- Xu, X., Tabuada, P., Grizzle, J.W., and Ames, A.D. (2015). Robustness of control barrier functions for safety critical control. *IFAC-PapersOnLine*, 48(27), 54–61.

⁴ The point-to-set distance is defined as $\|z\|_{\mathcal{A}} \triangleq \inf_{y \in \mathcal{A}} \|z - y\|$, where $\|\cdot\|$ is the standard Euclidean norm